

Optimal Synthesis of Reconfigurable Planar Arrays with Simplified Architectures for Monopulse Radar Applications

P. Rocca and A. F. Morabito

Abstract—A new approach to the power synthesis of fixed-geometry reconfigurable planar arrays radiating sum and difference patterns is presented. The proposed design technique allows to maximize the radiation performance (field slope, amplitude, or even directivity) of both beam patterns over assigned directions subject to completely arbitrary masks for sidelobe bounds. Whatever the elements disposal and the array boundary, the overall problem is solved through a convex (quadratic) programming procedure. Moreover, if centrosymmetric antenna layouts are adopted, the synthesis is reduced to an even more powerful linear programming routine which preserves the solution uniqueness and optimality guaranteed by quadratic programming codes while dramatically decreasing their computational weight (and hence enabling the design of much larger planar arrays). The proposed approach also takes into account the need of reducing the complexity of the beam forming network (*BFN*), which is fulfilled by sharing part of the excitation amplitudes between the two radiation modalities. A set of numerical examples is reported and discussed to show the versatility and effectiveness of the proposed approach.

Index Terms—Reconfigurable Arrays, Sum and Difference Patterns, Monopulse Antennas, Convex Programming Array Design.

I. INTRODUCTION

Monopulse radars are systems used to track the position of moving targets [1][2]. In order to avoid problems related to the power fluctuations of the backscattered signal (i.e., echo) due to the finite amount of time in which the target is illuminated by the transmitted pulse, monopulse radars are based on the short-term observation of the target echo and on the comparison of two different signals, the so-called sum and difference signals [1]. Towards this aim, monopulse antennas are required to provide both sum and a difference patterns [3], the former having one main lobe along the target direction and the latter exhibiting a null in the same direction. In case of linear phased arrays, the antenna is split into two parts, symmetric with respect to the center. Whether the two halves are excited in phase, a sum pattern is obtained. On the contrary, a difference pattern is generated when the two parts are excited in phase reversal, namely with a phase shift of π [1]. However,

linear arrays allow to track targets only on a plane. To enable the three-dimensional tracking, planar arrays are needed. In this case, the antenna has to generate one sum pattern and two difference patterns respectively exploited for estimating the azimuth and elevation coordinates identifying the target direction. The sum and difference patterns are obtained by subdividing the planar array into four symmetric quadrants: the sum mode is generated when all quadrants are excited with the same phase, while the two difference patterns are obtained by adding a phase shift of π to the excitations of a couple of quadrants. More precisely, the shift is added to the upper or lower quadrants for the elevation angle estimation and to left or right quadrants for the azimuthal angle estimation.

Notably, the excitation coefficients proving the two optimal radiation patterns can be so different [3] to require the adoption of two separate feeding networks. Unfortunately, this fact unavoidably increases the antenna complexity and costs. Hence, sub-optimal array solutions have been proposed in order to design affordable monopulse antennas. Among them, several approaches have been aimed at the design of compromise arrays generating an optimal sum beam, through independent excitations, and sub-optimal difference ones, by aggregating the elements into clusters/sub-arrays where each one is controlled by a single amplitude coefficients. In this framework, the design of both linear arrays [4][5][6][7][8] as well as planar arrays has been addressed [9][10] by using stochastic global optimization algorithms, deterministic as well as hybrid procedures. An interesting alternative solution for simplifying the *BFN* complexity, firstly explored in [11], regards the synthesis of sum and difference patterns while sharing some excitation weights between the two array modes. In particular, the synthesis of sum and difference patterns close as much as possible (in the least-square sense) to optimal Chebyshev (sum) [3] and Bayliss (difference) [3] patterns has been addressed in [11]. However, it is worth pointing out that the amplitudes of the central elements of optimal sum and difference patterns considerably differ while the elements in the periphery of the array (neglecting the phase shift needed for the difference mode generation) are similar.

On the basis of this observation, two design methods based on the Simulated Annealing [12] and the Genetic Algorithms [13] have been proposed for the design of linear arrays where the sum and difference modes have common amplitude excitations in the array tails. Unfortunately, such techniques turn out being relatively time consuming, especially when dealing with the synthesis planar arrays composed by a large

number of elements. Moreover, the achievement of the optimal compromise solution is not guaranteed due to the stochastic behavior of the resolution algorithms.

In the linear arrays case, these limitations have been overcome by the design technique presented in [14], which takes decisive advantage from the fundamental results of [15][16] and [17]. These contributions have definitively solved the optimal separate synthesis of fixed-geometry arrays radiating sum [15][16] and difference [17] power patterns with arbitrary sidelobe bounds by just exploiting convex programming (*CP*) routines, and hence result more effective and fast than the above-mentioned approaches. In particular, in [14] the array structure and the excitation amplitudes of the two radiation modalities are synthesized in such a way that a part of the weights in the periphery of the layout is shared between the two modes while the remaining elements have independent excitations, activated through a set of radio-frequency switches for generating either the sum or the difference beam. The synthesis problem has been again tackled by means of a procedure, with the inherent advantages in terms of solution optimality and computational complexity.

Taking into account such circumstances, this paper presents a new design approach providing four important contributions. First, it represents the extension of the method proposed in [14] to the case of two-dimensional reconfigurable monopulse arrays with arbitrary boundary. Second, differently from usual approaches dealing with reconfigurable fields, it provides to the designer several options in terms of cost functional to be optimized subject to arbitrary upper-bound constraints on the sidelobes, i.e.:

- the maximum sidelobe level of the sum pattern for a given beamwidth;
- the amplitude of the slope in the target direction of the difference pattern;
- the directivity of the sum and/or the difference beams.

As a third contribution, by exploiting the theory developed in [15][16][17] for the linear arrays case, this paper shows how the synthesis of a two-dimensional reconfigurable arrays radiating the sum and the two (azimuth and elevation) difference beams can be jointly addressed in a single optimization step and that the problem can be cast as a linear programming one provided that the radiating elements are disposed in a centrosymmetric fashion (whatever the layout boundary) with respect to the array center. Such a strategy is particularly suitable when dealing with the synthesis of planar arrays composed by a very large number of elements, as requested in challenging monopulse tracking applications. With respect to this point, it must be noted that while the reduction to *LP* already exists for the single objective problems, i.e., for the separate synthesis of sum or difference beams, its extension to reconfigurable sum and difference patterns is an innovation introduced by this paper. Finally, as fourth contribution, this work shows and discusses different techniques for the simplification of the array architecture, where common excitation amplitudes are considered on the external columns/rows of the array layout or on a complete ring of elements in the periphery of the antenna aperture. Moreover, it is proved

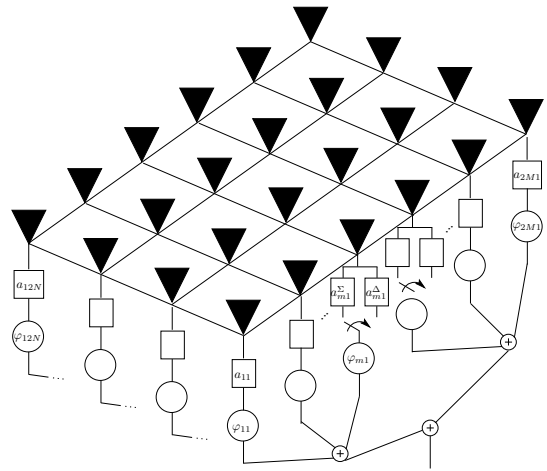


Fig. 1. Sketch of the planar antenna array generating sum and difference patterns with common and reconfigurable excitations.

that the proposed method can be naturally extended to the synthesis of hybrid architectures with common sub-arrays shared between the sum and difference modes.

The rest of the paper is organized as follows. The synthesis problem is mathematically formulated in Sect. II where the simplification of the *CP* problem to the *LP* one is also described. A set of numerical results is reported and discussed in Sect. III to show the potentialities and versatility of the proposed approach. Eventually, some conclusions are drawn in Sect. IV.

II. MATHEMATICAL FORMULATION

Let us consider a planar phased array made of $2M \times 2N$ isotropic sources distributed on a regular lattice centered in the $x - y$ plane as shown in Fig. 1. The radiated far-field is mathematically expressed through the array factor (*AF*) as

$$AF(u, v) = \sum_{m=1}^{2M} \sum_{n=1}^{2N} I_{mn} e^{j\beta[(m-M-\frac{1}{2})d_x u + (n-N-\frac{1}{2})d_y v]} \quad (1)$$

being $u = \sin \theta \cos \phi$, $v = \sin \theta \sin \phi$, $j = \sqrt{-1}$, $\beta = \frac{2\pi}{\lambda}$ (with λ the wavelength), and d_x and d_y are the element spacings along the x and y direction, respectively. Moreover, $I_{nm} = a_{mn} e^{j\varphi_{mn}}$, $m = 1, \dots, 2M$, $n = 1, \dots, 2N$ are the excitation weights, being a_{mn} and φ_{mn} the amplitude and phase coefficients of the mn -th element, respectively.

Supposing the phase shifters are only used for beam scanning purposes and set to $\varphi_{mn} = -\beta[(m-1)d_x u_0 + (n-1)d_y v_0]$, $m = 1, \dots, 2M$, $n = 1, \dots, 2N$, being (u_0, v_0) the direction where to steer the antenna pattern, let us assume in the following that the target direction is broadside: $(u_0, v_0) = (0, 0)$. The sum mode is generated by imposing a quadrantal symmetry of the excitation amplitudes, namely $a_{mn}^{\Sigma} = a_{(2M+1-m)n}^{\Sigma} = a_{m(2N+1-n)}^{\Sigma} = a_{(2M+1-m)(2N+1-n)}^{\Sigma}$, $m = 1, \dots, M$, $n = 1, \dots, N$. Accordingly, the array factor of

the sum (Σ) pattern turns out equal to [3]

$$AF^\Sigma(u, v) = 4 \sum_{m=1}^M \sum_{n=1}^N a_{mn}^\Sigma \cos \left[\left(m - M - \frac{1}{2} \right) d_x u \right] \times \cos \left[\left(n - N - \frac{1}{2} \right) d_y v \right] \quad (2)$$

where a_{mn}^Σ is the excitation amplitude of the mn -th element. The difference (Δ) mode is obtained by using a quadrantal anti-symmetric distribution of the amplitude weights. More specifically, the condition $a_{mn}^\Delta = a_{(2M+1-m)n}^\Delta = -a_{m(2N+1-n)}^\Delta = -a_{(2M+1-m)(2N+1-n)}^\Delta$ is considered to obtain a difference pattern for the azimuth angle estimation and the condition $a_{mn}^\Delta = -a_{(2M+1-m)n}^\Delta = a_{m(2N+1-n)}^\Delta = -a_{(2M+1-m)(2N+1-n)}^\Delta$ to generate the difference pattern for the elevation angle estimation [3]. The negative excitations are obtained by adding a phase shift of π to the signal received by corresponding quadrants. Hence, the two difference beams are defined as

$$AF_{az}^\Delta(u, v) = 4j \sum_{m=1}^M \sum_{n=1}^N a_{mn}^\Delta \sin \left[\left(m - M - \frac{1}{2} \right) d_x u \right] \times \cos \left[\left(n - N - \frac{1}{2} \right) d_y v \right] \quad (3)$$

$$AF_{el}^\Delta(u, v) = 4j \sum_{m=1}^M \sum_{n=1}^N a_{mn}^\Delta \cos \left[\left(m - M - \frac{1}{2} \right) d_x u \right] \times \sin \left[\left(n - N - \frac{1}{2} \right) d_y v \right]. \quad (4)$$

for the azimuthal and elevation Δ -mode, respectively.

A. Independent Synthesis of Sum and Difference Patterns

The set of coefficients generating optimal sum and difference patterns can be defined using for example analytical synthesis procedures (e.g., Taylor [18] and Bayliss [19]). In this work, the methods presented in [15][16] and [17] are exploited and integrated in a single design procedure aimed to jointly synthesize sum and difference patterns with shared excitations. By exploiting the theory reported in [15] and in [17], the optimal synthesis of the field (2) can be performed by solving the following *CP* problem:

$$\min_{\mathbf{a}^\Sigma} \left\{ -AF^\Sigma(u_0, v_0) \right\} \quad (5)$$

subject to

$$\left| AF^\Sigma(u_s, v_s) \right|^2 \leq UB^\Sigma(u_s, v_s) \quad s = 1, \dots, S \quad (6)$$

provided that the phase of the sum field in the target direction is equal to zero, where $\mathbf{a}^\Sigma = \{a_{mn}^\Sigma; m = 1, \dots, M; n = 1, \dots, N\}$ and $UB^\Sigma(u_s, v_s)$ is a non-negative function identifying an arbitrary upper bound on the sidelobes, (u_s, v_s) , $s = 1, \dots, S$ being the directions spanning the sidelobe region. By following the same principle,

the optimal design of difference patterns has been obtained by solving the following *CP* problem [17]:

$$\min_{\mathbf{a}^\Delta} \left\{ \left[-j \frac{\partial AF_{az/el}^\Delta(u, v)}{\partial w} \right] \Big|_{u=u_0; v=v_0} \right\} \quad (7)$$

subject to

$$AF_{az/el}^\Delta(u_0, v_0) = 0 \quad (8)$$

and

$$\left| AF_{az/el}^\Delta(u_s, v_s) \right|^2 \leq UB_{az/el}^\Delta(u_s, v_s) \quad s = 1, \dots, S \quad (9)$$

provided that the phase of the imaginary part of the difference field derivative in the target direction is equal to π , where $\mathbf{a}^\Delta = \{a_{mn}^\Delta; m = 1, \dots, M; n = 1, \dots, N\}$, w is either u or v depending on the kind of difference pattern to be synthesized, for azimuth ($w = u$) or elevation ($w = v$) angle estimation, the subscript $\{az/el\}$ refers to the consideration of the azimuth and/or of the elevation patterns, and $UB_{az/el}^\Delta(u_s, v_s)$ is the non-negative mask function on the sidelobes.

Due to the fact that (2) and (3)-(4) are purely real or imaginary functions, the quadratic constraints (6) and (9) can be reduced to linear ones as

$$-\sqrt{UB^\Sigma(u_s, v_s)} \leq AF^\Sigma(u_s, v_s) \leq \sqrt{UB^\Sigma(u_s, v_s)} \quad s = 1, \dots, S \quad (10)$$

$$-\sqrt{UB_{az/el}^\Delta(u_s, v_s)} \leq j AF_{az/el}^\Delta(u_s, v_s) \leq \sqrt{UB_{az/el}^\Delta(u_s, v_s)} \quad s = 1, \dots, S \quad (11)$$

for the sum and difference mode, respectively. Therefore, since the objective functions (5)(7) are linear with respect to the unknowns (see *Appendix*) each synthesis consists in the minimization of a linear function in a linear set and can be solved as a *LP* problem (see [16][17] for further details).

As a final comment (which must be also taken into account in reading the following Section), it is worth noting that looking just for the array excitation amplitudes (instead of both the real and imaginary part of the weights) represents neither a restrictive hypothesis nor a limitation which may affect the convexity of the optimization problem above. In fact, for both cases of continuous or discrete (i.e., array) sources, independently from the aperture size and contour, it is well known that the optimal source corresponding to a given sum pattern is a real and positive distribution [18][15][16]. Except for a π phase shift with respect to the aperture center, this property is also valid for the optimal source radiating a given difference pattern [19][17].

B. Joint Synthesis of Sum and Difference Patterns with Common Excitations

From a mathematical point of view, the fact of sharing a subset of the excitations between the sum and difference modes means that the condition

$$a_{mn}^\Sigma = a_{mn}^\Delta, (m, n) \in \Psi \quad (12)$$

is verified, Ψ being the set of integer couples identifying the elements with common weights. It is important to point out that (12) represents a linear constraint that can be added to the separate synthesis of sum and difference patterns discussed in the previous section. Regarding the solution procedure, condition (12) means that the number of unknown is reduced of a quantity equal to the cardinality of Ψ . Practically, a unique amplifier/attenuator, common between the Σ and Δ mode, should be used for each element in Ψ (Fig. 1). However, the joint synthesis of the sum and difference patterns have to be addressed. Accordingly, the method proposed in [14] is here customized to the planar array case and redefined as a *LP* resolution problem. More specifically, the monopulse array design problem is formulated as the definition of the two sets of coefficients \mathbf{a}^Σ and \mathbf{a}^Δ such that

$$\min_{\mathbf{a}^\Delta} \left\{ \left[-j \frac{\partial AF_{az}^\Delta(u, v)}{\partial u} \right] \Big|_{u=u_0; v=v_0} \right\} \quad (13)$$

subject to

$$AF_{az}^\Delta(u_0, v_0) = 0 \quad (14)$$

$$-AF^\Sigma(u_0, v_0) \leq -\eta \quad (15)$$

$$-\sqrt{UB^\Sigma(u_s, v_s)} \leq AF^\Sigma(u_s, v_s) \leq \sqrt{UB^\Sigma(u_s, v_s)} \quad (16)$$

$$-\sqrt{UB_{az}^\Delta(u_s, v_s)} \leq jAF_{az}^\Delta(u_s, v_s) \leq \sqrt{UB_{az}^\Delta(u_s, v_s)} \quad (17)$$

$$a_{mn}^\Sigma = a_{mn}^\Delta, (m, n) \in \Psi \quad (18)$$

where η is either a user-defined threshold or a parameter to be optimized. This constant represents a crucial parameter of the overall optimization, as it forces the amplitude value of the far-field pattern in the sum modality to exceed a prescribed level. In the test cases shown in Section III, the η value and the sidelobe upper-bound function have been jointly set in such a way to achieve a desired peak sidelobe level performance.

Since both the objective function (13) and all constraints (15)(16)(17)(18) are linear, the problem can be solved by using a *LP* solution procedure. Therefore, unless radiation constraints result so strict to prevent the existence of a solution, the globally optimal solution is unique and the fast convergence of the proposed procedure to it is guaranteed. It is worth noting that the joint problem is aimed to maximize the derivative of the difference pattern (i.e., slope) through (13) while the optimization of the sum beam is included as a constraint (15). The inversion of (13) and (15), aiming at maximizing the pencil beam amplitude subject to a lower bound constraint on the difference beam slope in the target direction, is also feasible. Moreover, in case also the optimization of the elevation Δ -pattern is required, the two following constraints have to be added

$$\left[-j \frac{\partial AF_{el}^\Delta(u, v)}{\partial v} \right] \Big|_{u=u_0; v=v_0} \leq -\kappa \quad (19)$$

$$AF_{el}^\Delta(u_0, v_0) = 0 \quad (20)$$

$$-\sqrt{UB_{el}^\Delta(u_s, v_s)} \leq jAF_{el}^\Delta(u_s, v_s) \leq \sqrt{UB_{el}^\Delta(u_s, v_s)} \quad (21)$$

$$s = 1, \dots, S$$

Notably, since the *LP* approach already exists just for the separate synthesis of sum or difference patterns, the adoption of *LP* to design planar arrays with reconfigurable sum and difference patterns can be considered as an innovation. Moreover, as the unique condition enabling the reduction to *LP* is the centrosymmetry of the array elements locations, this formulation is extremely powerful and can be adopted in a huge number of synthesis scenarios. In fact, all the properties of the approach hold true independently from the array boundary and the excitation shapes, even allowing the fast synthesis of aperiodic arrays. In the sum patterns case, this property is due to the fact that if a field is solution then its complex conjugate is a solution as well as long the array is centrosymmetric (as a conjugation in the far field domain corresponds to conjugation and specular reflection in the other domain). As the set of solutions is convex, the midpoint amongst the two field solutions, which is a real field, is a solution as well. Reality of array excitations follow [16]. Analogous reasonings hold true in the difference patterns case, where one can easily prove with the same tools that the array optimal excitations are purely imaginary (and hence a simple phase shift achieves the result one needs) [17]. The reduction of the overall synthesis to a *LP* problem allows one to dramatically enhances the procedure performance even with respect to the original quadratic programming (*QP*) approach. In fact, when comparing different convex programming routines, as the solutions optimality is anyway guaranteed, the crucial parameter which measures the actual effectiveness of a synthesis routine is its computational time [16][17]. The latter, in the present case, is uniquely determined by the number of array elements, and hence switching from quadratic to linear programming becomes decisive in all the applications wherein large planar arrays are required. These situations practically include all the synthesis scenarios wherein narrow beams and high resolutions are required, which is indeed the case in several satellite, radio astronomy, radar, and biomedical applications.

To further reduce the complexity of the antenna structure, the use of shared sub-arrays can be also taken into account. The synthesis of clusters of elements can be simply addressed by means of the proposed *LP*-based approach, by including as additional constraint

$$a_{mn}^\Sigma = a_{pq}^\Sigma \quad (22)$$

$$(m, n), (p, q) \in \Psi, (m, n) \neq (p, q)$$

or in dual fashion on the difference mode excitations as

$$a_{mn}^\Delta = a_{pq}^\Delta \quad (23)$$

$$(m, n), (p, q) \in \Psi, (m, n) \neq (p, q)$$

which forces the elements within a sub-array to have the same excitation value.

In support of the usefulness of the overall synthesis approach, two final observations must be done. First, the whole theory can be exploited in connection with the design procedure proposed in [20] in order to devise an innovative and

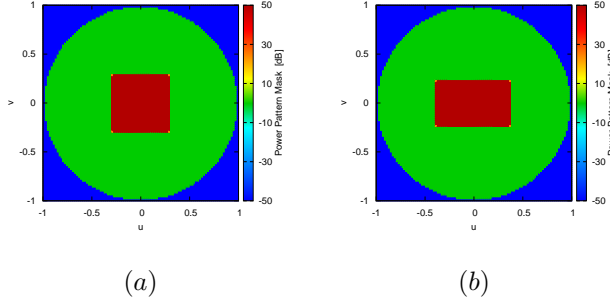


Fig. 2. *Example 1 - Staircase Mask* - ($M = N = 5$, $d_x = d_y = \frac{\lambda}{2}$, $\chi = [20, 40]\%$) - Behavior of the power mask (a) for the sum $[UB^\Sigma(u, v)]$ and (b) the difference $[UB^\Delta(u, v)]$ pattern.

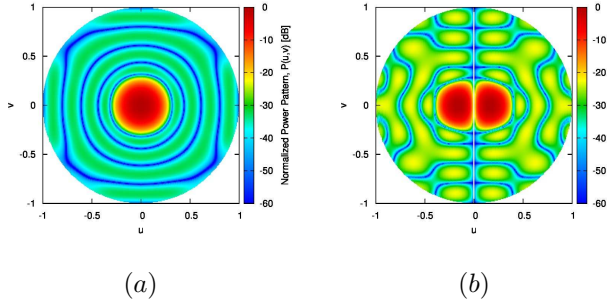


Fig. 3. *Example 1 - Staircase Mask* - ($M = N = 5$, $d_x = d_y = \frac{\lambda}{2}$, $\chi = 20\%$) - Power pattern for (a) the sum $[|AF^\Sigma(u, v)|^2]$ and (b) the azimuthal difference $[|AF_{az}^\Delta(u, v)|^2]$ mode synthesized by means of the proposed *LP*-based method with $\chi = 20\%$ common elements.

effective approach to the synthesis of reconfigurable planar arrays generating sum, difference, and shaped beams. Second, if the number of the array elements is not very large, so that the designer may renounce to *LP* formulation and adopt a *QP* approach, the optimization of the antenna directivity can be added to the optimization problem above. In this case, it should be necessary to consider the radiated powers in the sum modality

$$P^\Sigma = \int_0^{2\pi} \int_0^\pi |AF^\Sigma(\theta, \phi)|^2 \sin\theta d\theta d\phi \quad (24)$$

and in the difference modalities

$$P_{el}^\Delta = \int_0^{2\pi} \int_0^\pi |AF_{el}^\Delta(\theta, \phi)|^2 \sin\theta d\theta d\phi \quad (25)$$

$$P_{az}^\Delta = \int_0^{2\pi} \int_0^\pi |AF_{az}^\Delta(\theta, \phi)|^2 \sin\theta d\theta d\phi \quad (26)$$

and adding in the overall problem the convex constraints

$$P^\Sigma \leq \rho \quad (27)$$

$$P_{el}^\Delta \leq \sigma \quad (28)$$

$$P_{az}^\Delta \leq \tau \quad (29)$$

wherein ρ , σ , and τ are user-defined real and positive constants. Then, in order to enhance the directivity in the different

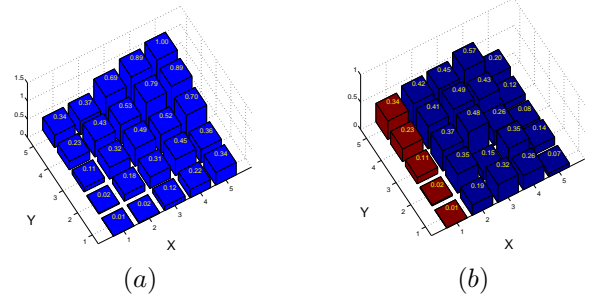


Fig. 4. *Example 1 - Staircase Mask* - ($M = N = 5$, $d_x = d_y = \frac{\lambda}{2}$, $\chi = 20\%$) - Excitation amplitudes of (a) the sum $[a^\Sigma]$ and (b) the azimuthal difference $[a_{az}^\Delta]$ mode synthesized by means of the proposed *LP*-based method with $\chi = 20\%$ common elements.

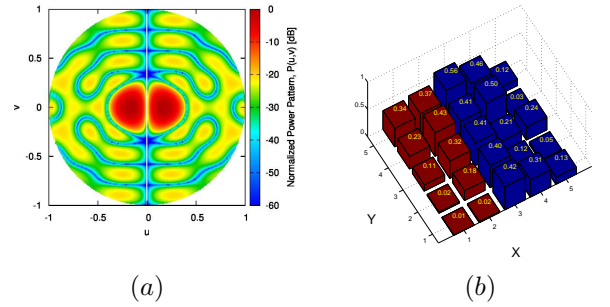


Fig. 5. *Example 1 - Staircase Mask* - ($M = N = 5$, $d_x = d_y = \frac{\lambda}{2}$, $\chi = 40\%$) - Plot of (a) the power pattern for the azimuthal difference mode $[|AF_{az}^\Delta(u, v)|^2]$ and (b) corresponding excitation amplitudes synthesized by means of the proposed *LP*-based method with $\chi = 40\%$ common elements.

modalities it should be necessary to solve the overall problem by choosing very small values of ρ , σ , and τ . As an alternative, the functional

$$P = P^\Sigma + P_{el}^\Delta + P_{az}^\Delta \quad (30)$$

should be minimized in place of (13), the latter being converted into a constraint having the same form of (19).

III. NUMERICAL RESULTS

The effectiveness and versatility of the proposed synthesis method are assessed in the following by considering a set of synthesis problems where different constraints (i.e., on the power masks and on the common weights) are imposed in the array design. As far as the adopted minimization algorithm is concerned, the MATLAB subroutine *linprog* has been adopted.

In the first example (*Example 1*), a planar array with $2M \times 2N = 10 \times 10$ elements has been taken into account with an inter-element distance along the x and y axis equal to $d_x = d_y = 0.5$. The power pattern masks for the sum and the

TABLE I

Example 1 - Staircase Mask - ($M = N = 5$, $d_x = d_y = \frac{\lambda}{2}$, $\chi = [20, 40] \%$) - FEATURES OF THE SUM AND DIFFERENCE POWER PATTERNS SYNTHESIZED BY MEANS OF THE PROPOSED LP -BASED METHOD WITH $\chi = 20\%$ AND $\chi = 40\%$ COMMON ELEMENTS.

	Σ - mode	Δ - mode
$\chi = 20\%$		
$Fitness$	41.3	135.0
$SLL [dB]$	-32.3	-22.8
$HPBW_u [rad]$	0.28	0.22
$HPBW_v [rad]$	0.28	0.28
$\chi = 40\%$		
$Fitness$	41.3	100.3
$SLL [dB]$	-32.3	-20.3
$HPBW_u [rad]$	0.28	0.24
$HPBW_v [rad]$	0.28	0.28

azimuthal difference modes¹, used as constraints in the LP -based optimization stage, are shown in Fig. 2(a) and Fig. 2(b), respectively, and have been discretized considering a number of samples equal to $S = 10 \times (2N \times 2M)$. The minimum requested value for the sum pattern fitness has been set to $\eta = 40$. Moreover, two columns of common elements have been imposed, namely $a_{mn}^\Sigma = a_{mn}^\Delta$ for $m = 1, \dots, M = 10$ and $n = 1$ and $n = N = 10$, such that $\chi = 20\%$ amplitude coefficients are shared between the sum and difference modes. The power patterns synthesized by means of the LP approach are given in Fig. 3. The corresponding amplitude excitations are reported in Fig. 4, where the common excitations are highlighted with a different color in Fig. 4(b). For the sake of clarity, only one quadrant of the excitation weights is shown in Fig. 4 by virtue of the quadrantal symmetry of the antenna. As it can be seen in Fig. 3, the sum pattern has very low sidelobes with a maximum sidelobe level $SLL^\Sigma = -32.3$ dB, while the difference mode has reasonably low sidelobes (i.e., $SLL^\Delta|_{\chi=20\%} = -22.8$ dB). The values of the half-power beamwidth ($HPWB$) along the u and v coordinate for the main lobe of the sum pattern and for one of the two main lobes of the difference pattern are reported in Tab. I as well. Moreover, the fitness values of the sum and difference patterns, namely $AF^\Sigma(u_0, v_0)$ and $\left[\frac{\partial AF_{\alpha z}^\Delta(u, v)}{\partial u}\right]_{u=u_0; v=v_0}$, for the best solution achieved at the end of the optimization procedure are also given in Tab. I. The simulation has been concluded in 9.7 [sec] using a standard processing unit (i.e., 2.4GHz PC with 2GB of RAM).

In order to investigate the possibility of further reducing the antenna complexity, another synthesis has been performed by fixing the sum pattern as in the previous case and optimizing the difference pattern imposing four columns of common elements (i.e., $a_{mn}^\Sigma = a_{mn}^\Delta$ for $m = 1, \dots, M = 10$ and $n =$

¹The synthesis problems have taken into account azimuthal difference patterns only. The inclusion of the elevation difference pattern in the synthesis process is straightforward and does not affect neither the generality nor the effectiveness of the proposed approach. Due to the 'centrosymmetry' constraints enforced on the excitations, once the optimal excitations corresponding to the azimuthal difference pattern have been identified, the unique operation to do in order to generate the elevation difference pattern is to add a 180 degrees shift to the phase of the excitations belonging to two non-adjacent quadrants of the array layout.

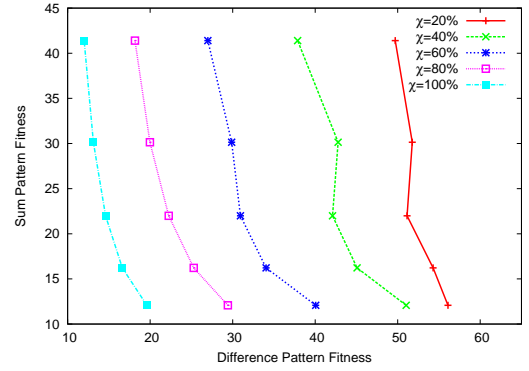


Fig. 6. Example 1 - Staircase Mask - ($M = N = 5$, $d_x = d_y = \frac{\lambda}{2}$, $\chi \in [20, 100] \%$) - Values of the fitness for the sum $[AF^\Sigma(u_0, v_0)]$ and difference pattern $\left[\frac{\partial AF_{\alpha z}^\Delta(u, v)}{\partial u}\right]_{u=u_0; v=v_0}$ for different reconfigurable arrays synthesized by means of the proposed LP -based method by varying design parameters (i.e., percentage of common elements and value of η).

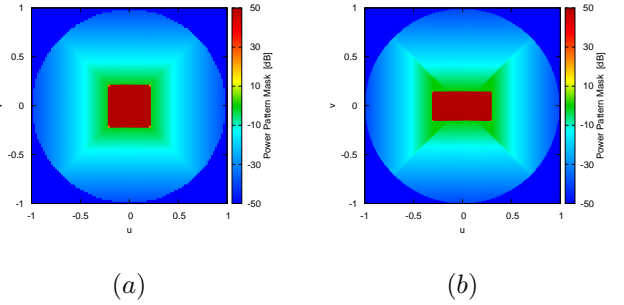


Fig. 7. Example 2 - Linearly-decreasing Mask - ($M = N = 5$, $d_x = d_y = \frac{\lambda}{2}$, $\chi = 20\%$) - Behavior of the power mask (a) for the sum $[UB^\Sigma(u, v)]$ and (b) the difference $[UB^\Delta(u, v)]$ pattern.

{1, 2, 9, 10} with $\chi = 40\%$ of common elements. The best solution achieved by means of the LP approach is given in Fig. 5. Due to the reduction of the number of unknowns in the optimization of the difference pattern, it is possible to observe in Fig. 5(a) that the level of the secondary lobes is higher with respect to the previous solution [Fig. 3(b)]. As a matter of fact, it turns out that $SLL^\Delta|_{\chi=40\%} = -20.3$ dB (Tab. I), 2.5 dB above the case with only $\chi = 20\%$ shared excitations. Moreover, also lower performance on the difference pattern fitness has been achieved (i.e., $\left[\frac{\partial AF_{\alpha z}^\Delta(u, v)}{\partial u}\right]_{\chi=40\%} = 100.3$ versus $\left[\frac{\partial AF_{\alpha z}^\Delta(u, v)}{\partial u}\right]_{\chi=20\%} = 135.0$) and broader major lobes with larger $HPBW$ (Tab. I). On the other side, the number of control points in the array architecture has been reduced of one fifth. The simulation stopped after 7.4 [sec], which proves again the computational lightness of the approach.

Following analogous reasonings, different synthesis problems have been optimally solved increasing the number of shared amplitude weights up to $\chi = 60\%$, $\chi = 80\%$, and also considering the case with all common amplifiers ($\chi = 100\%$). Successively, also the requested minimum performance on the sum pattern has been changed by varying the value of η . Figure 6 shows the values of the best fitness for the

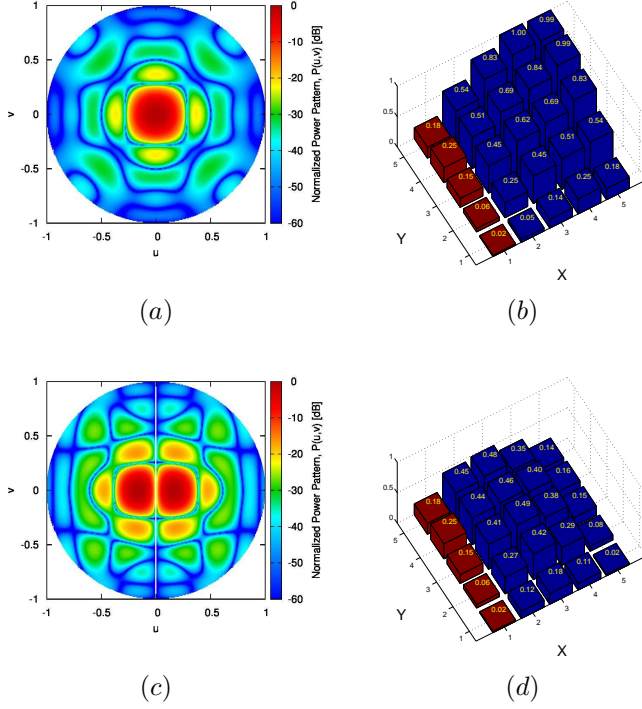


Fig. 8. *Example 2 - Linearly-decreasing Mask* - ($M = N = 5$, $d_x = d_y = \frac{\lambda}{2}$, $\chi = 20\%$) - Plot of (a)(c) the power pattern and (b)(d) the excitation amplitudes for (a)(b) the sum $[|AF^\Sigma(u, v)|^2, \mathbf{a}^\Sigma]$ and (b) the azimuthal difference $[|AF_{az}^\Delta(u, v)|^2, \mathbf{a}_{az}^\Delta]$ mode synthesized by means of the proposed *LP*-based method with $\chi = 20\%$ common elements.

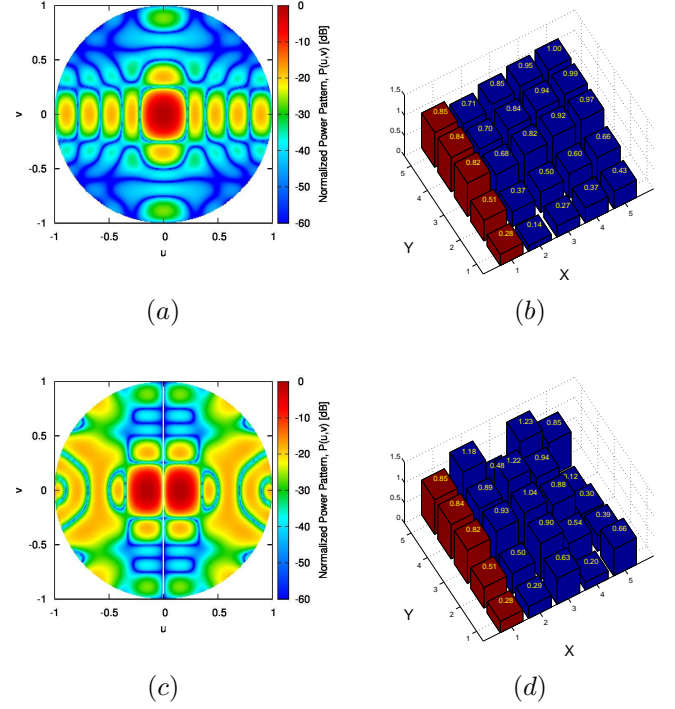


Fig. 10. *Example 2 - Sidelobe Depression* - ($M = N = 5$, $d_x = d_y = \frac{\lambda}{2}$, $\chi = 20\%$) - Plot of (a)(c) the power pattern and (b)(d) the excitation amplitudes for (a)(b) the sum $[|AF^\Sigma(u, v)|^2, \mathbf{a}^\Sigma]$ and (b) the azimuthal difference $[|AF_{az}^\Delta(u, v)|^2, \mathbf{a}_{az}^\Delta]$ mode synthesized by means of the proposed *LP*-based method with $\chi = 20\%$ common elements.

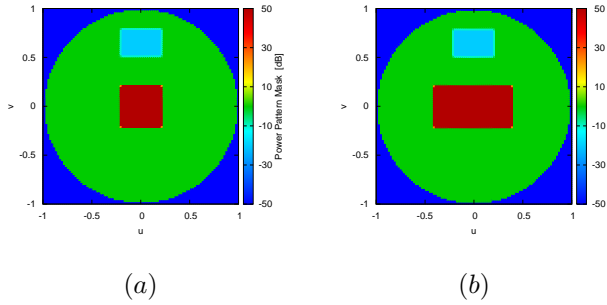


Fig. 9. *Example 2 - Sidelobe Depression* - ($M = N = 5$, $d_x = d_y = \frac{\lambda}{2}$, $\chi = 20\%$) - Behavior of the power mask (a) for the sum $[UB^\Sigma(u, v)]$ and (b) the difference $[UB^\Delta(u, v)]$ pattern.

Σ -mode and Δ -mode for the final solutions synthesized by means of the proposed approach. For a fixed sum pattern, it is possible to notice that the performance of the difference mode reduces as the percentage of the number of common elements increases. However, the difference pattern behavior can be ameliorated by imposing a less strict constraint on the requested sum pattern fitness. Hence, one of the key advantage of the proposed *LP*-based synthesis method is that of allowing the array designer to choose among the several optimal trade-off solutions according to the specific application at hand.

In the second example (*Example 2*), keeping the same antenna geometry of the previous case, the potentiality of the

proposed method has been investigated when varying the mask constraints on the secondary lobes. In particular, $UB^\Sigma(u, v)$ and $UB^\Delta(u, v)$ have been set such to force a decreasing behavior of the sidelobes [Figs. 7 and 8] and to obtain a sidelobe depression [Figs. 9 and 10] in a specific angular region. In both cases, the number of common elements between the sum and difference mode has been set to $\chi = 20\%$. The amplitude weights \mathbf{a}^Σ and \mathbf{a}^Δ for the optimal solution achieved at the end of the *LP*-based minimization when considering the masks of Fig. 7 are shown in Fig. 8(b) and 8(d), respectively. The corresponding power patterns, shown in Figs. 8(a) and 8(c), are characterized by the features summarized in Tab. II. As expected, the amplitude of the secondary lobes decreases as moving away from the main lobe peak direction. On the contrary, the peak sidelobe for both the sum and the difference mode ($SLL^\Sigma = -21.5 \text{ dB}$ and $SLL^\Delta = -16.5 \text{ dB}$) is higher with respect to the previous case, where a uniform level of the secondary lobes has been considered. In the second case, a depression of 20 dB below the sidelobe level has been imposed for the angular direction having $u \in [-0.2, 0.2]$ and $v \in [0.5, 0.8]$ (Fig. 9). The effectiveness of the approach is evident from the results shown in Fig. 10. Although the use of $\chi = 20\%$ shared excitations, the sidelobe depression has been correctly synthesized in both the sum power pattern [Fig. 10(a)] and the difference power pattern [Fig. 10(c)]. It is also important to notice that another depression has been obtained for direction (u, v) having $u \in [-0.2, 0.2]$

TABLE II

Example 2 - Linearly-decreasing Mask and Sidelobe Depression -
 $(M = N = 5, d_x = d_y = \frac{\lambda}{2}, \chi = 20\%)$ - FEATURES OF THE SUM AND
DIFFERENCE POWER PATTERNS SYNTHESIZED BY MEANS OF THE
PROPOSED *LP*-BASED METHOD WITH $\chi = 20\%$ WHEN CONSIDERING A
LINEARLY DECREASING MASK IN THE SIDELOBES AND A SIDELobe
DEPRESSION.

	$\Sigma - mode$	$\Delta - mode$
<i>Linearly decreasing mask</i>		
<i>Fitness</i>	48.1	36.0
<i>SLL</i> [dB]	-21.5	-16.5
<i>HPBW_u</i> [rad]	0.28	0.20
<i>HPBW_v</i> [rad]	0.28	0.24
<i>Sidelobe depression</i>		
<i>Fitness</i>	68.4	84.0
<i>SLL</i> [dB]	-17.9	-17.9
<i>HPBW_u</i> [rad]	0.24	0.22
<i>HPBW_v</i> [rad]	0.28	0.28

and $v \in [-0.8, -0.5]$ because of the adopted quadrantal excitation symmetry. In both cases, the final solution has been synthesized in less than 10 [sec].

The third example (*Example 3*) is aimed on the one hand at demonstrating the validity of the proposed approach to the design of reconfigurable sum and difference arrays with circular boundaries (i.e., a non-rectangular shape) and on the other hand at showing the results of a design of an array with layout similar to that considered in [16] and [17]. Accordingly, the circular aperture has been generated by imposing to zero the excitations of the elements outside a circular contour of radius 2.25λ as shown in Figs. 11(b) and 11(d). By assuming the same mask constraints of *Example 1* and imposing as common elements those of the two outer columns on each side of the array (i.e., 4 common elements amongst 17 for each quadrant such that $\chi \simeq 24\%$), the power patterns of the sum and difference beam synthesized by means of the proposed *LP*-based approach are reported in Figs. 11(a) and 11(c), respectively, while the corresponding excitation weights are given in Figs. 11(b) and 11(d). Although the levels of the secondary lobes unavoidably increase ($SLL^\Sigma = -20.0$ dB and $SLL^\Delta = -16.8$ dB) as compared to *Example 1* because of the reduced number of elements, it is important to observe that the method allows to keep both common weights between the two pattern as well as the circular aperture shape thus demonstrating the versatility of the approach to deal with array having arbitrary boundaries. Regarding the comparison with [16] and [17], although an array with the same layout is not present in the two reference works as instead required for the design of a reconfigurable sum-difference planar array, a planar array with $2M \times 2N = 14 \times 14$ and $d_x = d_y = 0.5$ is used which has been considered in [17] and is also very close to another array taken into account in [16]. The power masks imposed on the sum and difference patterns are reported in Fig. 12 and the results of the synthesis are shown in Fig. 13 where it is possible to observe that four columns of common elements have been imposed in the design (i.e., $\chi \simeq 35\%$). Outside the main lobe region identified by the mask constraints, the following peak values of the secondary

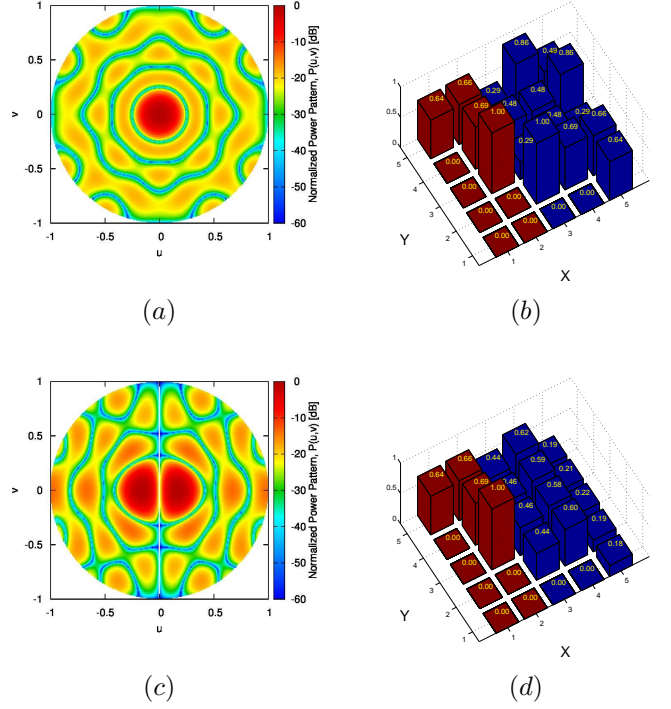


Fig. 11. *Example 3 - Circular Array -* $(M = N = 5, d_x = d_y = \frac{\lambda}{2}, \chi \simeq 24\%)$ - Plot of (a)(c) the power pattern and (b)(d) the excitation amplitudes for (a)(b) the sum $[AF^\Sigma(u, v)]^2$, \mathbf{a}^Σ and (b) the azimuthal difference $[AF^\Delta(u, v)]^2$, \mathbf{a}^Δ mode synthesized by means of the proposed *LP*-based method with $\chi \simeq 24\%$ of common elements.

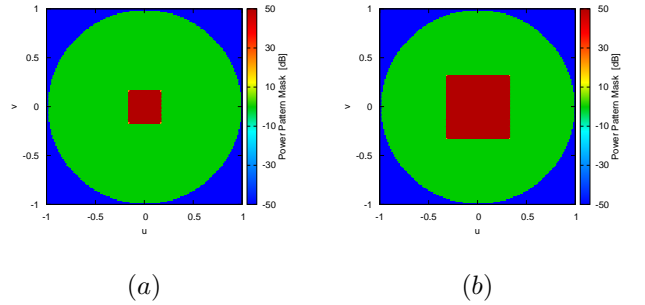


Fig. 12. *Example 3 - Comparison -* $(M = N = 7, d_x = d_y = \frac{\lambda}{2}, \chi \simeq 35\%)$ - Behavior of the power mask (a) for the sum $[UB^\Sigma(u, v)]$ and (b) the difference $[UB^\Delta(u, v)]$ pattern.

lobes have been achieved: $SLL^\Sigma = -24.8$ dB and $SLL^\Delta = -26.6$ dB. Although the same patterns of [16] and [17] can not be attained due to the use of common amplitude weights, the proposed approach is able to achieve solutions with close performance.

Finally and unlike the two previous examples, in the last example (*Example 4*) the simplification of the array architecture is obtained by imposing a ring of common elements and by using sub-arrays of four elements in the array tails. In the former case (“ring of common elements”), the same array of the previous examples is taken into account and the power pattern masks are characterized by a linearly decreasing

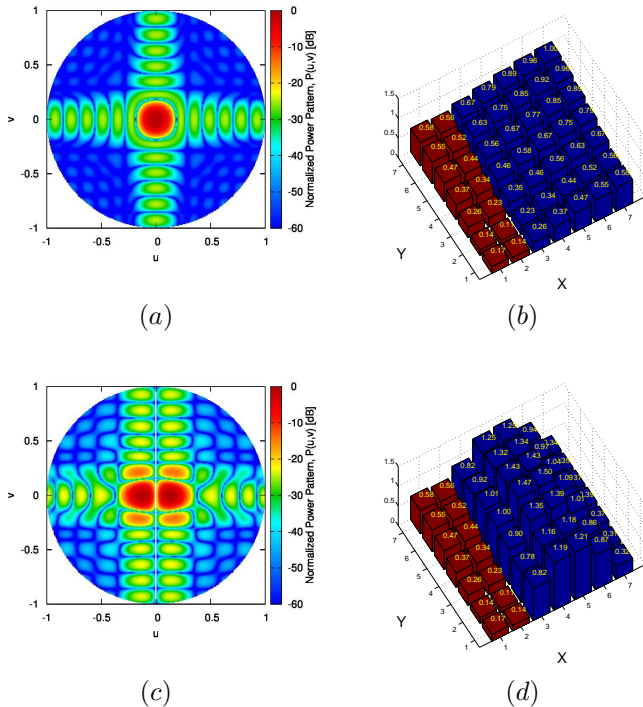


Fig. 13. *Example 3 - Comparison* - ($M = N = 7$, $d_x = d_y = \frac{\lambda}{2}$, $\chi \simeq 35\%$) - Plot of (a)(c) the power pattern and (b)(d) the excitation amplitudes for (a)(b) the sum $[|AF^\Sigma(u, v)|^2, \mathbf{a}^\Sigma]$ and (b) the azimuthal difference $[|AF_{az}^\Delta(u, v)|^2, \mathbf{a}_{az}^\Delta]$ mode synthesized by means of the proposed *LP*-based method with $\chi \simeq 35\%$ of common elements.

behavior. The two optimized sets of amplitude excitations, \mathbf{a}^Σ and \mathbf{a}_{az}^Δ , are shown in Figs. 14(b) and 14(d), respectively. The corresponding power patterns for the sum $|AF^\Sigma(u, v)|^2$ and the azimuthal difference $|AF_{az}^\Delta(u, v)|^2$ mode are given in Figs. 14(a) and 14(c). In the latter case (“*common sub-arrays*”), a larger array having $2M \times 2N = 12 \times 12$ elements is considered and each quadrant is characterized by 3 square sub-arrays of four elements. As for the power pattern bounds, staircase masks with equal amplitude constraints on the sidelobe region are taken into account. The final solution is shown in Fig. 15 where the optimized excitation weights for the sum and the difference patterns are reported in Figs. 15(b) and 15(d), respectively. Whether on the one hand it is evident that the sub-arrayed layout of the common amplitude coefficients has been achieved with a consequent array simplification, on the other hand the large number of common elements penalizes the difference pattern performance with peak sidelobes at $SLL^\Delta = -15.4 \text{ dB}$ unlike the sum pattern having $SLL^\Sigma = -23.0 \text{ dB}$ (Tab. III).

IV. CONCLUSIONS

A new method for the synthesis of planar arrays generating optimal sum and difference patterns with arbitrary sidelobe bounds and sharing a sub-set of the excitation weights has been presented. The problem has been formulated as a mask-constrained power pattern synthesis and the use of common excitations in the periphery of the array aperture, has allowed

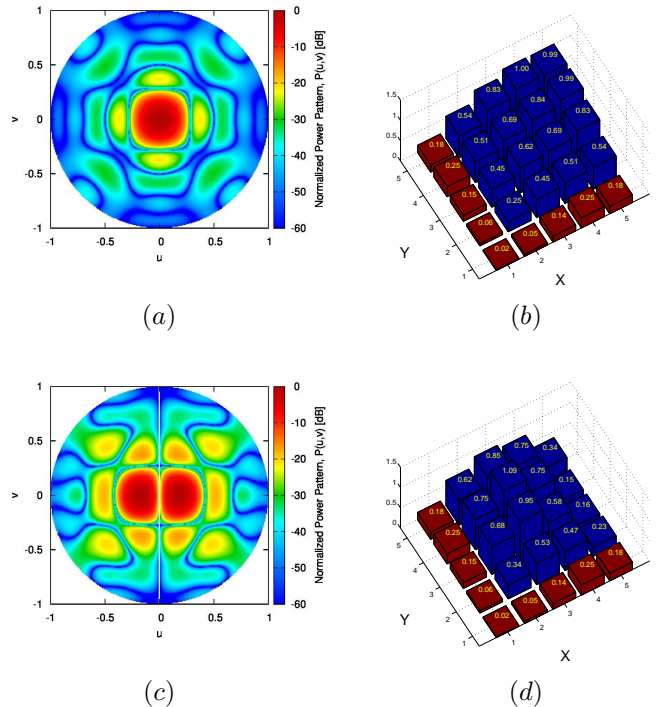


Fig. 14. *Example 4 - Ring of Common Elements* - ($M = N = 5$, $d_x = d_y = \frac{\lambda}{2}$, $\chi = 20\%$) - Plot of (a)(c) the power pattern and (b)(d) the excitation amplitudes for (a)(b) the sum $[|AF^\Sigma(u, v)|^2, \mathbf{a}^\Sigma]$ and (b) the azimuthal difference $[|AF_{az}^\Delta(u, v)|^2, \mathbf{a}_{az}^\Delta]$ mode synthesized by means of the proposed *LP*-based method with the outer ring of common elements.

a reduction of the overall array complexity while still guaranteeing an optimal radiation performance. Notably, it has been demonstrated that the problem of the joint design of sum and difference power patterns can be addressed, under symmetric array layout conditions, by means of a linear programming procedure, much simpler with respect to the convex programming strategy already proposed in the literature. The reported results have shown the effectiveness of the proposed technique in achieving final results satisfying the user defined constraints. The versatility of the design approach has been pointed out by considering very heterogeneous power pattern masks as well as different array architectures (also having partial sub-arrayed layout). Thanks to the use of the linear programming procedure, the synthesis of planar arrays for monopulse radar applications has been addressed with a computational burden similar to the one needed by the *CP* approach for linear arrays having a number of element one order of magnitude below. Furthermore, the effectiveness of the proposed approach has been also assessed through comparisons with benchmark procedures able to guarantee the achievement of provably optimal solutions in the separate synthesis of sum and difference patterns.

APPENDIX

The proof that the objective functions (5) and (7) are linear with respect to the problem unknowns, \mathbf{a}_{mn}^Σ and \mathbf{a}_{mn}^Δ respectively, is here reported. As for the Σ -mode, the objective

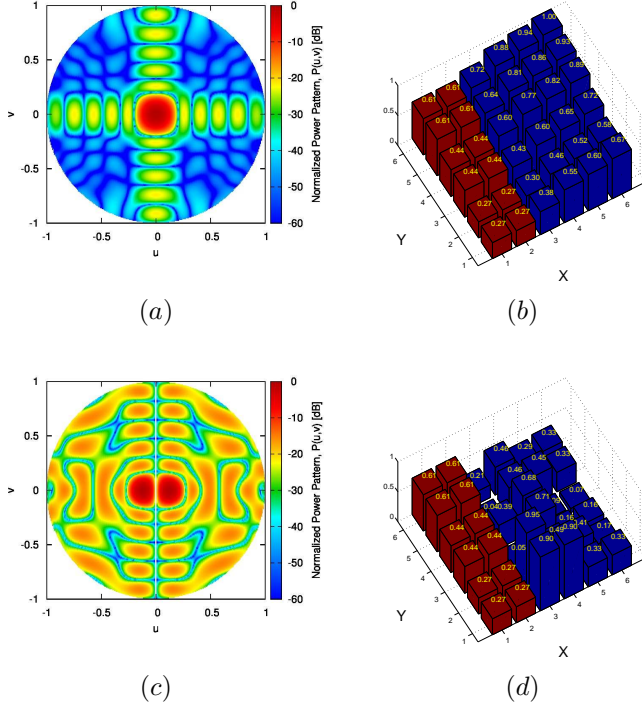


Fig. 15. Example 4 - Common Sub-arrays - ($M = N = 6$, $d_x = d_y = \frac{\lambda}{2}$, $\chi = 33\%$) - Plot of (a)(c) the power pattern and (b)(d) the excitation amplitudes for (a)(b) the sum $[|AF^\Sigma(u, v)|^2, \mathbf{a}^\Sigma]$ and (c)(d) the azimuthal difference $[|AF_{az}^\Delta(u, v)|^2, \mathbf{a}_{az}^\Delta]$ mode synthesized by means of the proposed LP-based method with common sub-arrays.

function is equivalent to the array factor computed along the boresight direction (u_0, v_0) with the sign inverted, namely

$$-AF^\Sigma(u_0, v_0) = -4 \sum_{m=1}^M \sum_{n=1}^N a_{mn}^\Sigma \times \cos \left[\left(m - M - \frac{1}{2} \right) d_x u_0 \right] \cos \left[\left(n - N - \frac{1}{2} \right) d_y v_0 \right] \quad (31)$$

that is linear with respect to the coefficients a_{mn}^Σ , $m = 1, \dots, M$, $n = 1, \dots, N$.

Regarding the Δ -mode and considering the azimuthal pattern (dual analysis holds true for the elevation pattern), the objective function is given by (7)

$$\left[\frac{\partial AF_{az}^\Delta(u, v)}{\partial u} \right] \Big|_{u=u_0; v=v_0} \quad (32)$$

where the derivative of $AF_{az}^\Delta(u, v)$ computed along u and evaluated in (u_0, v_0) is equal to

$$\left[\frac{\partial AF_{az}^\Delta(u, v)}{\partial u} \right] \Big|_{u=u_0; v=v_0} = 4j \sum_{m=1}^M \sum_{n=1}^N a_{mn}^\Delta \left(m - M - \frac{1}{2} \right) \times d_x \cos \left[\left(m - M - \frac{1}{2} \right) d_x u_0 \right] \cos \left[\left(n - N - \frac{1}{2} \right) d_y v_0 \right]$$

which is linear with respect to a_{mn}^Δ , $m = 1, \dots, M$, $n = 1, \dots, N$.

REFERENCES

[1] S. M. Sherman and D. K. Barton, *Monopulse Principles and Techniques* (2nd Ed.). Norwood, MA: Artech House, 2011.
 [2] M. I. Skolnik, *Radar Handbook* (3rd Ed.). New York, NY: McGraw-Hill, 2008.

TABLE III

Example 4 - Ring of Common Elements and Common Sub-arrays - ($M = N = \{5, 6\}$, $d_x = d_y = \frac{\lambda}{2}$, $\chi = \{36, 33\} \%$) - FEATURES OF THE SUM AND DIFFERENCE POWER PATTERNS SYNTHESIZED BY MEANS OF THE PROPOSED LP-BASED METHOD WHEN CONSIDERING A RING OF COMMON ELEMENTS AND COMMON SUB-ARRAYS IN THE ARRAY TAILS.

	Σ - mode	Δ - mode
<i>Ring of common elements</i>		
<i>Fitness</i>	48.1	16.4
<i>SLL [dB]</i>	-20.4	-16.8
<i>HPBW_u [rad]</i>	0.28	0.24
<i>HPBW_v [rad]</i>	0.28	0.28
<i>Common sub-arrays</i>		
<i>Fitness</i>	86.4	51.5
<i>SLL [dB]</i>	-23.0	-15.4
<i>HPBW_u [rad]</i>	0.18	0.15
<i>HPBW_v [rad]</i>	0.18	0.18

[3] R. S. Elliott, *Antenna Theory and Design*. Hoboken, NJ: Wiley & Sons., 2003.
 [4] P. Lopez, J. A. Rodriguez, F. Ares, and E. Moreno, "Subarray weighting for difference patterns of monopulse antennas: Joint optimization of subarray configurations and weights," *IEEE Trans. Antennas Propag.*, vol. 49, no. 11, pp. 1606-1608, Nov. 2001.
 [5] S. Caorsi, A. Massa, M. Pastorino, and A. Randazzo, "Optimization of the difference patterns for monopulse antennas by a hybrid real/integer coded differential evolution method," *IEEE Trans. Antennas Propag.*, vol. 53, no. 1, pp. 372-376, Jan. 2005.
 [6] M. D'Urso, T. Isernia, and E. F. Meliadd, "An effective hybrid approach for the optimal synthesis of monopulse antennas," *IEEE Trans. Antennas Propag.*, vol. 55, no. 4, pp. 1059-1066, Apr. 2007.
 [7] L. Manica, P. Rocca, A. Martini, and A. Massa, "An innovative approach based on a tree-searching algorithm for the optimal matching of independently optimum sum and difference excitations," *IEEE Trans. Antennas Propag.*, vol. 56, no. 1, pp. 58-66, Jan. 2008.
 [8] Y. Chen, S. Yang, and Z. Nie, "The application of a modified differential evolution strategy to some array pattern synthesis problems," *IEEE Trans. Antennas Propag.*, vol. 56, no. 7, pp. 1919-1927, Jul. 2008.
 [9] F. Ares, J. A. Rodriguez, E. Moreno, and S. R. Rengarajan, "Optimal compromise among sum and difference patterns," *J. Electromagn. Waves Appl.*, vol. 10, pp. 1543-1555, 1996.
 [10] L. Manica, P. Rocca, M. Benedetti, and A. Massa, "A fast graph-searching algorithm enabling the efficient synthesis of sub-arrayed planar monopulse antennas," *IEEE Trans. Antennas Propag.*, vol. 57, no. 3, pp. 652-663, Mar. 2009.
 [11] T. Lee, and T. Tseng, "Subarray-synthesized low-side-lobe sum and difference patterns with partial common weights," *IEEE Trans. Antennas Propag.*, vol. 41, no. 6, pp. 791-800, Jun. 1993.
 [12] M. Alvarez-Folgueiras, J. Rodriguez-Gonzales, and F. Ares-Pena, "Synthesizing Taylor and Bayliss linear distributions with common aperture tail," *Electron. Lett.*, vol. 45, no. 11, pp. 18-19, 2009.
 [13] M. Alvarez-Folgueiras, J. Rodriguez-Gonzales, and F. Ares-Pena, "Optimal compromise among sum and difference patterns in monopulse antennas: Use of subarrays and distributions with common aperture tail," *J. Electromagn. Waves Appl.*, vol. 23, pp. 2301-2311, 2009.
 [14] A. Morabito, and P. Rocca, "Optimal synthesis of sum and difference patterns with arbitrary sidelobes subject to common excitations constraints," *IEEE Antennas Wireless Propag. Lett.*, vol. 9, pp. 623-626, 2010.
 [15] T. Isernia, P. Di Iorio, and F. Soldovieri, "An effective approach for the optimal focusing of array fields subject to arbitrary upper bounds," *IEEE Trans. Antennas Propag.*, vol. 48, no. 12, pp. 1837-1847, Dec. 2000.
 [16] O. M. Bucci, L. Caccavale, and T. Isernia, "Optimal far-field focusing of uniformly spaced arrays subject to arbitrary upper bounds in nontarget directions," *IEEE Trans. Antennas Propag.*, vol. 50, no. 11, pp. 1539-1554, Nov. 2002.
 [17] O. M. Bucci, M. D'Urso, and T. Isernia, "Optimal synthesis of difference patterns subject to arbitrary sidelobe bounds by using arbitrary array antennas," *IEE Proc. Microw. Antennas Propag.*, vol. 152, no. 3, pp. 129-137, 2005.
 [18] T. T. Taylor, "Design of a circular apertures for narrow beamwidth and

low sidelobe," *Trans. IRE Antennas Propag.*, vol. 8, no 1, pp. 17-22, Jan. 1960.

- [19] E. T. Bayliss, "Design of monopulse antenna difference patterns with low sidelobes," *Bell System Tech. Journal*, vol. 47, pp. 623-640, 1968.
- [20] A. F. Morabito, A. Massa, P. Rocca, and T. Isernia, "An effective approach to the synthesis of phase-only reconfigurable linear arrays," *IEEE Trans. Antennas Propag.*, vol. 60, n. 8, pp. 3622-3631, Aug. 2012.